

Neighborhood Structure Assisted Non-negative Matrix Factorization and its Application in Unsupervised Point Anomaly Detection

Imtiaz Ahmed

IMTIAZAVI@TAMU.EDU

*Department of Industrial and Systems Engineering
Texas A & M University
College Station, TX, USA*

Xia Ben Hu

HU@CSE.TAMU.EDU

*Department of Computer Science and Engineering
Texas A & M University
College Station, TX, USA*

Mithun P. Acharya

MITHUN.ACHARYA@US.ABB.COM

*Lead Principal Scientist
ABB Corporate Research
Raleigh, NC, USA*

Yu Ding

YUDING@TAMU.EDU

*Department of Industrial and Systems Engineering
Texas A & M University
College Station, TX, USA*

Editor: Francis Bach, David Blei, and Bernhard Schölkopf

Abstract

Dimensionality reduction is considered as an important step for ensuring competitive performance in unsupervised learning such as anomaly detection. Non-negative matrix factorization (NMF) is a popular and widely used method to accomplish this goal. But NMF, together with its recent, enhanced version, like graph regularized NMF or symmetric NMF, do not have the provision to include the neighborhood structure information and, as a result, may fail to provide satisfactory performance in presence of nonlinear manifold structure. To address that shortcoming, we propose to consider and incorporate the neighborhood structural similarity information within the NMF framework by modeling the data through a minimum spanning tree. What motivates our choice is the understanding that in the presence of complicated data structure, a minimum spanning tree can approximate the intrinsic distance between two data points better than a simple Euclidean distance does, and consequently, it constitutes a more reasonable basis for differentiating anomalies from the normal class data. We label the resulting method as the neighborhood structure assisted NMF. By comparing the formulation and properties of the neighborhood structure assisted NMF with other versions of NMF including graph regularized NMF and symmetric NMF, it is apparent that the inclusion of the neighborhood structure information using minimum spanning tree makes a key difference. We further devise both offline and online algorithmic versions of the proposed method. Empirical comparisons using twenty benchmark datasets as well as an industrial dataset extracted from a hydropower plant

demonstrate the superiority of the neighborhood structure assisted NMF and support our claim of merit.

Keywords: Minimum Spanning Tree, Non-negative Matrix Factorization, Unsupervised Anomaly Detection

1. Introduction

Matrix factorization (MF) is one popular framework for finding the low dimensional embedding in a high dimensional dataset. MF based approaches have been employed successfully to represent and group high dimensional data for better learning capability. Methods which can be described using the traditional matrix factorization framework such as the principal component analysis (PCA) produces low rank matrices consisting of negative values and positive and negative weights, which tends to cancel each other in reconstructing the original matrix, and hence provides no intuitive meaning. The non-negative matrix factorization (Lee and Seung, 1999, NMF) method, which imposes the non-negativity constraint in matrix factorization and only allows additive linear combinations of components, comes out as a better candidate for finding the low dimensional representation of high dimensional data. NMF has the capability of generating both clustering assignments and meaningful attribute distribution in two separate matrices. Immediately after its introduction, NMF not only becomes a powerful tool for clustering (Xu et al., 2003), but it also shows enough potential in anomaly detection (Allan et al., 2008; Tong and Lin, 2011; Liu et al., 2017).

In the presence of complicated manifolds, however, researchers notice that NMF starts to lose its efficiency (Kuang et al., 2012; Cai et al., 2011) as it only tries to approximate the data without trying to mimic the similarity among observations in the latent space. In other words, the shortcoming of the original NMF is attributed to that it has no provision to include the neighborhood structure information during the calculation of the factored matrices and thus cannot approximate the manifold embedded in the data.

Our research finds it beneficial to include the structural similarity information of data, along with the original attribute information, in the objective function of an NMF-based method. Our specific approach is as follows. First, we convert the original data matrix into a graph object where each node represents an observation and each edge represents the virtual connection between a pair of data points. Then we apply a minimum spanning tree (Prim, 1957, MST) on the graph to build a similarity matrix which is sparse and thus leading to computational efficiency. This MST-based similarity matrix also has the advantage to approximate the manifold structure of a local neighborhood (Costa and Hero, 2003), better than simple Euclidean distances could. Our previous effort (Ahmed et al., 2019a) shows that making use of the neighborhood structure through a MST model indeed helps the objective of anomaly detection, but this previous effort, Ahmed et al. (2019a), does not involve the matrix factorization framework and its formulation is *ad hoc*.

We refer to the resulting method in this paper as the neighborhood structure-assisted NMF (NS-NMF). We demonstrate the benefit of the neighborhood structure-assisted NMF in the task of anomaly detection. Our study will show that clustering benefits in low dimensional space and consideration of the local invariance property in obtaining those clusters make neighborhood structure-assisted NMF a powerful anomaly detection method.

We want to note that two recent versions of the NMF method are closely related to what we propose in this paper. One of them is the graph regularized NMF (Cai et al., 2011, GNMF), which regularizes the original NMF formulation using a Laplacian matrix. Different from the proposed neighborhood structure-assisted NMF, GNMF constructs the similarity matrix based on simple Euclidean distances. Our numerical testing shows furthermore that GNMF, when employed for anomaly detection, is rather sensitive to two of its tuning parameters: the number of nearest neighbors and a regularization parameter. By contrast, the neighborhood structure-assisted NMF does not need the neighborhood parameter and its detection outcome appears to be much less sensitive to its regularization parameter. The second NMF variant is the symmetric NMF (Kuang et al., 2012, SNMF), which uses only the similarity information while excluding the attribute information to generate the low rank matrices. In absence of the attribute information, SNMF depends on a dense pairwise similarity measure which leads to computational disadvantage unlike MST. By abandoning the original attribute information in its formulation, SNMF makes its detection outcomes less interpretable or ‘meaningful’ than NS-NMF or GNMF. Comparing the neighborhood structure-assisted NMF with other versions of NMF (plain NMF, GNMF and SNMF) over 20 benchmark datasets shows a clear and evident advantage of the proposed method.

To root our development in the background of anomaly detection, we would like to note that anomaly detection is related naturally to *clustering*, as researchers argue that detecting anomalies is to separate the data points into two classes—normal or regular versus abnormal, irregular, or anomalous (Ester et al., 1996; Ertöz et al., 2004; Yu et al., 2002; Otey et al., 2003; He et al., 2003; Amer and Goldstein, 2012). NMF based (or rather, all MF based) methods fall under the umbrella of clustering based approaches as they also try to group the data in the low dimensional feature space, which appears to be in line with the subspace based methods advocated for anomaly detection (Zhang et al., 2004; Kriegel et al., 2009; Zimek et al., 2012; Müller et al., 2008; Keller et al., 2012; Van Stein et al., 2016).

The major contributions of our research reported here can be summarized as follows. First, we propose and design a new objective function, which incorporates neighborhood similarity information, to be used in the NMF framework for conducting data dimension reduction and data grouping. This neighborhood structure assisted NMF is the central piece in our subsequent anomaly detection procedure. Second, we compare the formulation and properties of the neighborhood structure assisted NMF with other variants of NMF (GNMF and SNMF) and highlight the similarities and differences between them. This provides an in-depth understanding of how the neighborhood structure assisted NMF makes a difference in anomaly detection. Last but not the least, we provide both offline and online algorithmic implementations of the proposed neighborhood structure assisted NMF method to enhance its practical usefulness.

The rest of the paper unfolds as follows. Section 2 describes the detailed formulation of the neighborhood structure assisted NMF. Section 3 discusses the similarities and differences among the proposed approach, GNMF and SNMF. Section 4 presents the proposed NS-NMF algorithm in a structured way for both offline and online versions. Section 5 compares the proposed NS-NMF method with other NMF variants on 20 benchmark datasets. We also apply these methods to a hydropower dataset. Finally, we summarize the paper in Section 6.

2. Neighborhood Structure Assisted NMF and its Application in Anomaly Detection

Anomaly detection is by and large an unsupervised learning problem as the class labels of data records are unknown in the training set and one has to depend on the structure of the data to flag a potential anomaly. Anomalies could be *global* and lie far away from most of the data points thus making it easy to identify them, or it could be *local* and homogeneously co-exist around the regular data points and only be found if compared with proper neighboring set/clusters. Nonetheless, to differentiate the anomalies from the normal background one may need to solve two problems. The first is to find the appropriate local contexts/communities as latent feature groups and their respective members, and the second is to extract the standard characteristics of these communities in terms of the original features so that they can serve as a basis for comparison. We use these communities to compare and judge all the data points for flagging and short listing potential anomalies. NMF apparently provides an effective solution to both of these problems. However, as we have pointed out earlier, the traditional NMF framework does not take into consideration the neighborhood structure of the data points while doing clustering in latent space and thereby produce unsatisfactory results. Also, approximating the neighborhood structure in presence of non linear manifold is not straightforward either. In this section, we try to bridge this knowledge gap by proposing a graph based approach to approximate the neighborhood structure and develop a new neighborhood structure assisted NMF formulation for anomaly detection. The formulation consider the local invariance property while obtaining the low dimensional representation and thus should intuitively work better than the competing approaches.

2.1 Basic NMF Framework

In NMF (Lee and Seung, 1999), a data matrix $\mathbf{A} \in \mathbb{R}_+^{n \times p}$, of which columns and rows represent the attributes and observations respectively, is factorized into two low rank matrices, namely, $\mathbf{W} \in \mathbb{R}_+^{n \times K}$ and $\mathbf{H} \in \mathbb{R}_+^{K \times p}$, such that the inner product of these factorized matrices approximate the original data matrix. Here, K represents the number of latent feature groups and it is required to be equal or less than the smaller of n and p . NMF tries to project the data with high dimensional features into a low dimensional latent space so that the original observations can be seen as a weighted linear combination of the newly formed basis vectors corresponding to each latent feature group. The rows of \mathbf{H} , each of which is a $1 \times p$ vector, represent the basis vectors, whereas the weights come from \mathbf{W} . For example, any row i from the original matrix can be reconstructed through (1) below:

$$\mathbf{a}_i = \sum_{k=1}^K W_{ik} \mathbf{h}_k, \quad (1)$$

where \mathbf{a}_i represents the i -th row of \mathbf{A} , \mathbf{h}_k represents the k -th row of \mathbf{H} , and W_{ik} is the (i, k) -th element of \mathbf{W} .

To solve for the factored matrices, one needs to minimize the Frobenius norm of the difference between the original data matrix and the inner product of the factored matrices,

as shown in (2).

$$\min_{\mathbf{W} \geq \mathbf{0}, \mathbf{H} \geq \mathbf{0}} \|\mathbf{A} - \mathbf{WH}\|_F^2. \quad (2)$$

where $\|\cdot\|_F$ denotes the Frobenius norm and the constraints, $\mathbf{W} \geq \mathbf{0}$ and $\mathbf{H} \geq \mathbf{0}$, mean that both \mathbf{W} and \mathbf{H} are non-negative matrices.

2.2 Capturing Neighborhood Structure using MST

NMF finds its way in solving clustering problems when Ding et al. (2005) show that NMF can be made equivalent to clustering approaches by formulating in a different way. In other words, it turns out that if properly formulated, NMF could have the advantages of regular clustering frameworks. As mentioned earlier, while doing clustering, NMF does not consider neighborhood structure information. But the neighborhood structure information should have been considered for the benefit of clustering or detection, as structurally similar observations in the original space ought to maintain the similarity in the latent space. To tackle this problem, we propose to extract the neighborhood structure information from the original data matrix via the modeling of a minimum spanning tree and then incorporate the structure information during the calculation of the NMF factored matrices, so as to make the resulting method more suitable for anomaly detection.

To discover the intrinsic structure in data, a popular undertaking is to form a graph object using the original data matrix \mathbf{A} . Each observation is represented by a node, which is connected with other nodes through a weighted edge with the weight being the pairwise Euclidean distance between them. A simple graph like this has its disadvantage—the similarity matrix thus generated would be too dense to be incorporated in the NMF setting for large datasets. In our treatment, we instead use the MST for constructing the similarity matrix among data points, and doing so leads to a sparse similarity matrix.

To understand the concept of MST, consider a connected undirected graph $G = (V, E)$, where V is the collection of nodes and E represents the collection of edges connecting these vertices as pairs. For an edge $e \in E$, as mentioned above, a weight is associated with it, which is the pairwise Euclidean distance between the chosen pair of nodes. A minimum spanning tree is a subset of the edges in E that connects all the vertices together, without any cycles and with the minimum possible total edge weight. For more clear understanding, consider an example in Fig.1, left panel, where, there are 8 nodes and 15 edges connecting them in total. Each of the edges has a unique edge length associated with it which is represented by a numeric value. If we want to connect all the nodes using the given edges without forming a cycle, there could be many such combinations with only one having the minimum total edge length, which is shown in the right panel. The edges in black color represent the selected 7 edges from the 15 total edges. The resulting graph consists of the black edges only in the right panel is the MST for the initial connected graph. Apparently, MST compresses the original graph and preserves certain degree of information that we consider important for anomaly detection purpose.

Once we apply MST on the graph object resulting from the original data matrix \mathbf{A} having n observations, what we get is a square matrix, $\mathbf{M} \in \mathbb{R}_+^{n \times n}$, showing the pairwise connectedness and distance. A strictly positive value in \mathbf{M} represents the distance between two connected nodes in the resulting MST, whereas a zero indicates the disconnection between the two nodes. Different from the complete graph, \mathbf{M} of MST is supposed to be a

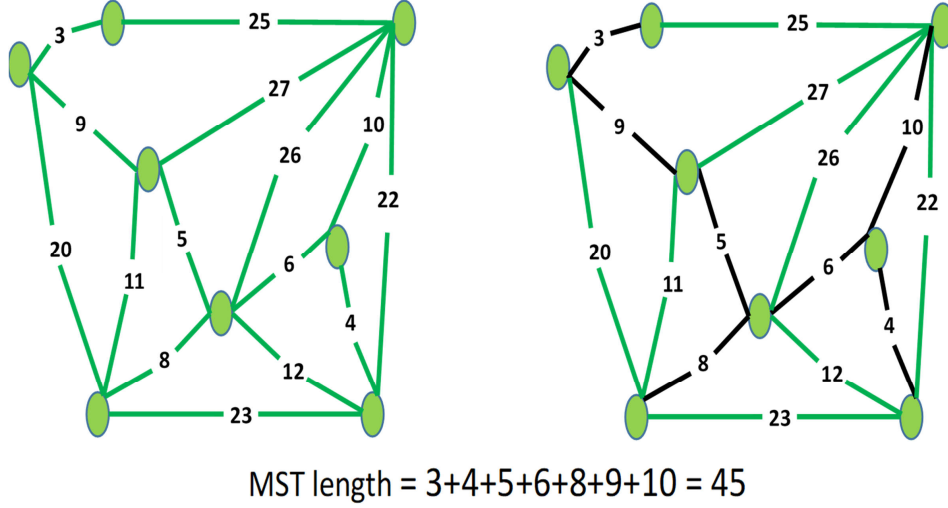


Figure 1: Formation of a MST: the left panel is the initial graph, and the black colored edges form the minimum spanning tree in the right panel.

sparse matrix, rather than a dense matrix. We further convert it into a pairwise similarity matrix, \mathbf{S} , by inverting only the positive entries of \mathbf{M} , as following:

$$S_{ij} = \begin{cases} \frac{1}{M_{ij}}, & \text{if } M_{ij} > 0, \\ 0, & \text{otherwise.} \end{cases}$$

where S_{ij} and M_{ij} are, respectively, the (i, j) -th elements of \mathbf{S} and \mathbf{M} . This matrix is called a similarity matrix because a high value in \mathbf{S} is the result of two nodes close to each other in the resulting MST, implying their similarity and likely the same cluster membership. On the other hand, a zero value means that two nodes are not directly connected and less likely similar to each other. Whether or not they may still belong to the same cluster depends largely on the two nodes' association with the common neighbors. Understandably, if two points have very low similarity and do not have connection through any common neighbors, they most probably belong to two separate clusters. Creating the similarity matrix is because we intend for \mathbf{S} to guide the basic NMF process to group the similar observations into the same cluster, obtain the proper cluster centroids in the form of basis vectors, and subsequently use the cluster centroids in the action of anomaly detections.

2.3 Proposed NS-NMF Formulation

By taking into account both the original attribute matrix \mathbf{A} and the MST based neighborhood similarity matrix \mathbf{S} , we propose the following NS-NMF formulation to obtain the low rank factored matrices \mathbf{W} and \mathbf{H} :

$$\min_{\mathbf{W} \geq \mathbf{0}, \mathbf{H} \geq \mathbf{0}} \|\mathbf{S} - \mathbf{W}\mathbf{W}^T\|_F^2 + \alpha \|\mathbf{A} - \mathbf{W}\mathbf{H}\|_F^2 + \gamma (\|\mathbf{W}\|_F^2 + \|\mathbf{H}\|_F^2), \quad (3)$$

where $\|\mathbf{W}\|_F^2$ and $\|\mathbf{H}\|_F^2$ are the regularization terms added to the objective function to avoid overfitting, γ is the regularization parameter controlling the extent of overfitting. The first term is apparently the newly added structure similarity term, whereas the second term is the original NMF cost function, and the parameter α is used to trade off between these two cost functions and takes values between 0 and 1.

The merit of NS-NMF is to make sure that data points coming from the same background or from the same neighborhood are grouped into the same cluster. NMF in its original setting only tries to find the basis vectors that best approximate the data. While NMF can achieve successes by doing so in the presence of simple Euclidean structure, it does not appear effective in the presence of complicated intrinsic data structure. In those cases NMF may achieve the data approximation objective but the clustering assignments may not be appropriate. But making proper clustering assignments is important for anomaly identification. As we see in (4), factoring out the right \mathbf{h}_k is the key piece for computing the anomaly score and plays a decisive role in the subsequent anomaly detection.

The MST-based neighborhood structure approximates the geodesic distance between data instances via the multi-hop edge connection on the tree graph, which are considered a much better representation of complicated data structures and similarity between data instances than simple Euclidean distances (Yu et al., 2015; Tu et al., 2016; Costa and Hero, 2003). The geodesic distance measures the minimum possible distance between two points in a curved space (like the surface of the earth), or more generally speaking, in a structured space. By incorporating the MST structural similarity measure in the NMF, the resulting method produces better clustering assignments with respective cluster centroids extracted from \mathbf{H} ; doing so, we believe, helps substantially the mission of anomaly detection.

2.4 Local Anomaly Detection

Now, let us take a look at how the proposed NS-NMF can help us in distinguishing anomalies from the normal observations. The low rank factored matrices generated from NS-NMF provide us with the information we are seeking to solve the two problems discussed at the beginning of this section pertinent to anomaly detection. Each entry of \mathbf{W} measures the extent of an observation’s association with all K latent groups/clusters, whereas a row of \mathbf{H} represents the average characteristics of one of the latent groups/clusters. To measure how an observation is deviating from its local context/group/community, we measure the Euclidean distance between the observation’s original attribute values and the average characteristics of that local community to which it belongs to. In other words, we create an anomaly score for observation i , which is calculated as in (4):

$$O_i = \|\mathbf{a}_i - \mathbf{h}_k\|_2 \quad \text{when observation } i \text{ belongs to local community } k. \quad (4)$$

We repeat this process for all observations and rank the scores, $\{O_i, i = 1, \dots, n\}$, in descending order.

In the practice of anomaly detection, it is common that once applied to the data, a method ranks the top N instances as potential anomalies and treats the rest of data instances as normal instances. One main reason for such a decision process is that unsupervised anomaly detection methods tend to have a lower detection capability and higher false alarm rate. As a result, unsupervised detection methods are typically used as a screening

tool, flagging potential anomalies to be further analyzed by either a human operator or some more expensive procedure. A cut-off is therefore used to ensure the subsequent, more expensive or time consuming step practical and feasible. In this paper, we follow this practice to declare the observations with top N scores as anomalies where the cut-off threshold N is prescribed based on the cost/feasibility considerations.

3. NS-NMF Relative to Other NMFs

In this section, we want to highlight the similarities and contrast of the proposed NS-NMF with some of the related approaches, principally GNMF and SNMF so that the readers get a better understanding of how the proposed method made the difference.

First, we present the formulations of the three methods in (5)–(7). To capture the essence of the NS-NMF method, we rewrite our original formulation in (3) by ignoring the third component of the objective function, because the third term is a regularization term to avoid overfitting, and as such, having it or not does not change the essence concerning which piece of information is used in the matrix factorization. The new formulation of NS-NMF in (7) now has two terms. We also change the position of α for easiness of comparison.

$$\text{GNMF} : \min_{\mathbf{W}, \mathbf{H} \geq \mathbf{0}} \lambda \cdot \text{tr}(\mathbf{W}^T \mathbf{L} \mathbf{W}) + \|\mathbf{A} - \mathbf{W} \mathbf{H}\|_F^2. \quad (5)$$

$$\text{SNMF} : \min_{\mathbf{W} \geq \mathbf{0}} \|\mathbf{S} - \mathbf{W} \mathbf{W}^T\|_F^2. \quad (6)$$

$$\text{NS-NMF} : \min_{\mathbf{W}, \mathbf{H} \geq \mathbf{0}} \frac{1}{\alpha} \cdot \|\mathbf{S} - \mathbf{W} \mathbf{W}^T\|_F^2 + \|\mathbf{A} - \mathbf{W} \mathbf{H}\|_F^2. \quad (7)$$

Conceptually and formulation wise, GNMF is the closest to the proposed NS-NMF. We notice that both NS-NMF and GNMF formulations have the same second component. This second component comes from the original NMF formulation and is used to obtain two factor matrices from the original data matrix, one of which is the attribute matrix.

Admittedly, the authors of GNMF are the first to shed light on the necessity of considering neighborhood similarity information in the original NMF process. According to Cai et al. (2011), the low rank approximation should be obtained as in (5), rather than in (2), in order to incorporate the neighborhood similarity information. The specific mechanism of incorporating the neighborhood similarity information in (5) is through the use of a graph Laplacian matrix, denoted by \mathbf{L} . The graph Laplacian matrix \mathbf{L} can be obtained by $\mathbf{L} = \mathbf{D} - \tilde{\mathbf{S}}$, where \mathbf{D} is a diagonal matrix also known as degree matrix (Cai et al., 2011; Ding et al., 2005) and $\tilde{\mathbf{S}}$ is the adjacency matrix. The adjacency matrix is calculated using the Euclidean structured neighborhood information after converting the original data into a graph object. The model has two main parameters, namely, q , the number of the nearest neighbors to be specified in order to form the similarity matrix, and, λ , the regularization parameter. The value of λ can take any non-negative value. When it takes the value of zero, the formulation ignores the neighborhood similarity completely and GNMF reduces to the original NMF.

SNMF, on the other hand, promotes the idea that one should probably consider the neighborhood similarity information only while obtaining the factored matrices. The factorization of the similarity matrix \mathbf{S} generates a clustering assignment matrix \mathbf{W} that is also constrained to be non-negative. The authors of SNMF believe that doing so captures

the inherent cluster structure from the graph representation of the original data matrix. Kuang et al. (2012) argue, and present case studies in support of, that the traditional NMF is not ideal for handling datasets with nonlinear structures. Compared to the plain NMF, SNMF can deal with complicated patterns and generate more accurate clustering assignments. Kuang et al. (2012) also point out that the SNMF formulation is in fact equivalent to some graph clustering methods including spectral clustering (Ding et al., 2005). Kuang et al. (2012) present an example to show that adding the non-negativity constraints help the clustering objective and also that SNMF performs more robustly compared to other clustering methods, as SNMF does not depend on the eigenvalue structure which tends to provide inaccurate results if certain conditions are violated.

SNMF formulation takes basically the first component of the NS-NMF formulation, because SNMF ignores the original NMF portion and uses the similarity information alone. SNMF focuses only on the accuracy of clustering assignments but for the mission of anomaly detection we need something more. What we need is to have a basis for comparison, so that we can pinpoint anomalies by looking at their deviation from the average characteristics of associated cluster. The second portion of the NS-NMF formulation helps us obtain a cluster centroid matrix which summarizes the attribute distribution of the latent feature groups, thereby providing the basis for detecting the anomalies from the clusters. For this reason, NS-NMF, which keeps the second term, is more meaningful for anomaly detection than SNMF. Even the first term, although appears the same in both SNMF and NS-NMF formulations, is not really the same, because the respective similarity matrix \mathbf{S} used therein is different. SNMF uses the traditional Euclidean distance based similarity metric considering the full graph, while that in NS-NMF comes from an MST. The similarity matrix in SNMF is too dense, making SNMF to suffer in case of approximating complex structures. Unsurprisingly, SNMF is computationally more expensive than NS-NMF.

Coming back to GNMF, which has the same second term as NS-NMF and poised to be more suitable for anomaly detection. The first term in both NS-NMF and GNMF formulations has a strong connection. It can be shown that when using the same similarity matrix \mathbf{S} , GNMF and NS-NMF can be made (nearly) equivalent.

To facilitate the understanding of this connection, let us consider adding an orthogonality constraint on \mathbf{W} . This is not exactly required in the original formulations but Ding et al. (2005) shows that minimizing $\|\mathbf{S} - \mathbf{W}\mathbf{W}^T\|_F^2$ retains the orthogonality of \mathbf{W} approximately. Suppose that the symmetric normalized Laplacian matrix is used, i.e., the original \mathbf{L} is pre- and post-multiplied by $\mathbf{D}^{-\frac{1}{2}}$, then we have

$$\mathbf{L} = \mathbf{I} - \mathbf{D}^{-\frac{1}{2}}\tilde{\mathbf{S}}\mathbf{D}^{-\frac{1}{2}},$$

where without ambiguity, we still use \mathbf{L} to denote the symmetric normalized Laplacian matrix. Furthermore, denote by $\mathbf{S} = \mathbf{D}^{-\frac{1}{2}}\tilde{\mathbf{S}}\mathbf{D}^{-\frac{1}{2}}$ the newly generated normalized similarity/adjacency matrix. As such, the first term in GNMF can be made equivalent to that of

NS-NMF by considering the following minimization formulation.

$$\begin{aligned}
 \min_{\mathbf{W} \geq \mathbf{0}} \text{tr}(\mathbf{W}^T \mathbf{L} \mathbf{W}) &= \min_{\mathbf{W} \geq \mathbf{0}} \text{tr}(\mathbf{W}^T (\mathbf{I} - \mathbf{D}^{-\frac{1}{2}} \tilde{\mathbf{S}} \mathbf{D}^{-\frac{1}{2}}) \mathbf{W}) \\
 &= \min_{\mathbf{W} \geq \mathbf{0}} \text{tr}(\mathbf{W}^T (\mathbf{I} - \mathbf{S}) \mathbf{W}) \\
 &= \min_{\mathbf{W} \geq \mathbf{0}} \text{tr}(\mathbf{W}^T \mathbf{W}) - \text{tr}(\mathbf{W}^T \mathbf{S} \mathbf{W}) \\
 &= \min_{\mathbf{W} \geq \mathbf{0}; \mathbf{W}^T \mathbf{W} = \mathbf{I}} \text{tr}(\mathbf{I}) - \text{tr}(\mathbf{W}^T \mathbf{S} \mathbf{W}).
 \end{aligned} \tag{8}$$

At the last expression, we use the orthogonality constraint on \mathbf{W} , as mentioned above. Minimizing (8) with respect to a non-negative \mathbf{W} does not change its minimization outcome if we add a term that does not depend on \mathbf{W} and multiply the \mathbf{W} -depending term by a constant. Let us add one term, $\text{tr}(\mathbf{S}^T \mathbf{S})$, to the last expression of (8) and multiply $\text{tr}(\mathbf{W}^T \mathbf{S} \mathbf{W})$ by two. As such, we end up with an equivalent minimization problem as follows:

$$\begin{aligned}
 \min_{\mathbf{W} \geq \mathbf{0}} \text{tr}(\mathbf{W}^T \mathbf{L} \mathbf{W}) \quad \text{is equivalent to} \quad & \min_{\mathbf{W} \geq \mathbf{0}; \mathbf{W}^T \mathbf{W} = \mathbf{I}} \text{tr}(\mathbf{I}) - 2\text{tr}(\mathbf{W}^T \mathbf{S} \mathbf{W}) + \text{tr}(\mathbf{S}^T \mathbf{S}) \\
 &= \min_{\mathbf{W} \geq \mathbf{0}; \mathbf{W}^T \mathbf{W} = \mathbf{I}} \text{tr}[(\mathbf{S} - \mathbf{W} \mathbf{W}^T)^T (\mathbf{S} - \mathbf{W} \mathbf{W}^T)] \\
 &= \min_{\mathbf{W} \geq \mathbf{0}; \mathbf{W}^T \mathbf{W} = \mathbf{I}} \|\mathbf{S} - \mathbf{W} \mathbf{W}^T\|_F^2.
 \end{aligned} \tag{9}$$

The above derivation makes it apparent that if one uses the same similarity matrix \mathbf{S} in both GNMF and NS-NMF formulations, then GNMF is practically the same as NS-NMF. Of course, which \mathbf{S} to use creates the difference between GNMF and NS-NMF. GNMF uses only a fixed small subset of the neighborhood/adjacency information to obtain an Euclidean distance based similarity matrix and then convert it to a graph Laplacian form. A prescribed neighborhood size, q , is one of the parameters used in GNMF. NS-NMF's similarity matrix, on the other hand, is based on an MST and differs from that of GNMF. NS-NMF does not need the neighborhood size parameter, due to its use of MST. Both methods use a regularization parameter, which is $\alpha(0 - 1)$ in NS-NMF and $\lambda(\geq 0)$ in GNMF; these regularization parameters are in fact equivalent. Our numerical analysis shows that GNMF is sensitive to both of its parameters, q and λ , while the NS-NMF is reasonably less sensitive to its parameter α . We believe that this is a benefit of using the MST-based similarity matrix.

4. Algorithmic Implementation of NS-NMF

In this section, we discuss the implementation of the formulation proposed in Section 2 in details. We provide two algorithmic procedures, one is an accelerated offline implementation, i.e., which process all the observations at the same time to evaluate their anomalousness and another is an online implementation, i.e., which process observations one at a time for real time anomaly detection.

4.1 Accelerated Offline Implementation

A number of algorithms have already been proposed to solve the original NMF problem and its variants. However, most of them are computationally expensive and not ideal for handling the big data scenario. In this paper, we choose to utilize a distributed version of the stochastic gradient descent (SGD) algorithm (Liu et al., 2017; Gemulla et al., 2011) which enables us to achieve an accelerated and parallel optimization scheme. In the traditional SGD, one updates the parameters at each round by going through a single training point at a time, whereas in the distributed version, we update the parameters by processing multiple independent blocks of training data in parallel and thereby taking the computational advantage. Here, independence means that parameter update of one block will not affect the parameter update of any other block, this property is also known as the interchangeable property (Liu et al., 2017; Gemulla et al., 2011). To design a distributed SGD, we define a loss function as in (10), which is just the block wise summation of the objective function defined in (3)

$$\begin{aligned}
 L_{\mathbf{S},\mathbf{A}}(\mathbf{W}, \mathbf{H}) &= \sum_{\{i,j,k\}} \left(\left\| \mathbf{S}^{ij} - \mathbf{W}^i \mathbf{W}^{jT} \right\|_F^2 + \frac{\gamma}{2B} \|\mathbf{W}^i\|_F^2 + \frac{\gamma}{2B} \|\mathbf{W}^j\|_F^2 \right. \\
 &\quad \left. + \frac{\alpha}{2} \left\| \mathbf{A}^{ik} - \mathbf{W}^i \mathbf{H}^{kT} \right\|_F^2 + \frac{\alpha}{2} \left\| \mathbf{A}^{jk} - \mathbf{W}^j \mathbf{H}^{kT} \right\|_F^2 + \frac{\gamma}{B} \|\mathbf{H}^k\|_F^2 \right) \quad (10) \\
 &= \sum_{\{i,j,k\}} L_{i,j,k}(\mathbf{W}^i, \mathbf{W}^j, \mathbf{H}^k).
 \end{aligned}$$

where B represents the number of splits in each dimension and it controls the number of blocks created in \mathbf{S} and \mathbf{A} . We essentially divide \mathbf{S} and \mathbf{A} into blocks and the position of each block is represented by the superscripts, i, j, k . Suppose that we have a 100×100 matrix and $B = 5$. Then we will have 5 blocks with each containing 400 (i.e., a 20×20 matrix) training points. To process and approximate a block \mathbf{S}^{ij} , we need to update parameter block \mathbf{W}^i and \mathbf{W}^j . Likewise, to approximate a block of \mathbf{A}^{ik} , we need to update \mathbf{W}^i and \mathbf{H}^k . As we have to process blocks from two separate matrices \mathbf{S} and \mathbf{A} , with parameters to be updated connecting each other, we define the blocks to be processed from these two matrices as an instance set $\{\mathbf{S}^{ij}, \mathbf{A}^{ik}, \mathbf{A}^{jk}\}$.

To achieve distributed and parallel processing, we need to process randomly generated instance sets at each round parallelly and it is possible only if they are interchangeable and as a result do not affect the resulting parameter updates $\{\mathbf{W}^i, \mathbf{W}^j, \mathbf{H}^k\}$ of one another. According to Gemulla et al. (2011), the interchangeability occurs only when the superscripts of the blocks do not coincide. For example, $\{\mathbf{S}^{15}, \mathbf{A}^{13}, \mathbf{A}^{53}\}$ and $\{\mathbf{S}^{23}, \mathbf{A}^{24}, \mathbf{A}^{34}\}$ are two interchangeable instances as they have entirely different superscripts. Now, as we have defined both the loss function and the instance sets, parameter update can be calculated according to (11) where $\theta^{i,j,k} = \{\mathbf{W}^i, \mathbf{W}^j, \mathbf{H}^k\}$ and ϵ_t is the step size at current iteration.

$$\theta_{t+1}^{i,j,k} = \theta_t^{i,j,k} - \epsilon_t \Delta L_{i,j,k}(\theta_t^{i,j,k}). \quad (11)$$

The algorithm steps is summarized in Algorithm 1, including the construction of MST based similarity matrix, the NMF optimization procedure, and the detection of anomalies.

Algorithm 1: Offline implementation of NS-NMF algorithm for anomaly detection

Input : \mathbf{A} , α , N , γ , B , K
Output: List of anomalous nodes l_{final}

- 1 Generate a set of vertices V , where each vertex represent a separate observation from the dataset;
- 2 Construct edges by calculating Euclidean distance between each pair of vertices using their attribute values from the dataset and store them in E ;
- 3 Construct a MST using V and E and generate the pairwise similarity matrix \mathbf{S} from the resultant pairwise MST distance matrix;
- 4 Initialize \mathbf{W} and \mathbf{H} randomly;
- 5 Partition \mathbf{S} and \mathbf{A} and corresponding \mathbf{W} and \mathbf{H} into blocks;
- 6 **while** *not converged* **do**
 - 7 Randomly generate a collection of instance sets from blocked \mathbf{S} and \mathbf{A} ,
 $U = \{\{i_1, j_1, k_1\}, \{i_2, j_2, k_2\}, \{i_3, j_3, k_3\}, \dots\}$ such that any two are interchangeable;
 - 8 **for** $(i, j, k) \in U$ *in parallel* **do**
 - 9 $\mathbf{W}'^i \leftarrow \mathbf{W}^i - \epsilon_t \Delta_{\mathbf{W}^i} L_{i,j,k}$;
 - 10 $\mathbf{W}'^j \leftarrow \mathbf{W}^j - \epsilon_t \Delta_{\mathbf{W}^j} L_{i,j,k}$ (if $i \neq j$);
 - 11 $\mathbf{H}'^k \leftarrow \mathbf{H}^k - \epsilon_t \Delta_{\mathbf{H}^k} L_{i,j,k}$;
 - 12 $\mathbf{W}^i \leftarrow \mathbf{W}'^i, \mathbf{W}^j \leftarrow \mathbf{W}'^j, \mathbf{H}^k \leftarrow \mathbf{H}'^k$;
 - 13 Non negativity projection for $\mathbf{W}^i, \mathbf{W}^j$ and \mathbf{H}^k ;
 - 14 **end**
- 15 **end**
- 16 **for** $k = 1 : K$ (*number of latent features*) **do**
 - 17 Make the clustering assignment according to the largest entry in each row of \mathbf{W} ;
 - 18 Calculate the local anomaly scores of the cluster members according to (4) and store them in O_i ;
- 19 **end**
- 20 Store the accumulated list of nodes with anomaly scores from all the clusters as
 $l_{total} = \{O_1, O_2, \dots, O_n\}$;
- 21 Return the nodes associated with top N local anomaly scores as final anomalies in
 l_{final} ;

4.2 Online Implementation

The offline implementation discussed above possess the advantage of parallel blockwise implementation but lacks the ability of instantaneous update and real-time anomaly score computing. It requires to see all the data at once and hence build the MST using all the instances even before the execution of the algorithm. To evaluate an observation in real time, we need to find a way to update both weight matrix \mathbf{W} and basis matrix \mathbf{H} incrementally when new samples arrive in a streaming fashion. In addition, we need to make sure that, such an update will not require the entire data matrix and the MST weights to reside in the memory.

There has been quite a few efforts in developing the online version of the plain NMF (Guan et al., 2012; Zhao and Tan, 2016; Zhu and Honeine, 2017; Tu et al., 2018; Guo and Zhang, 2019), although comparatively fewer attempts have been made in terms of online GNMF (Liu et al., 2016). It is so because adding geometric structures to guide the NMF process makes the online update more difficult as we need to calculate the geometric weights on the fly. In this section we layout the online implementation of NS-NMF.

Let us assume that the observations, $\mathbf{A} = [\mathbf{a}_1, \mathbf{a}_2, \dots, \mathbf{a}_{d-1}, \mathbf{a}_d]$, are generated in a streaming fashion, where \mathbf{a}_d represents the d th data sample just arrived and its attribute information. Upon its arrival, the d th component of the weight matrix and basis matrix need to be updated so that the instantaneous anomaly score can be calculated. For this d th data sample we can write our NS-NMF objective function by ignoring the regularization component as following:

$$\begin{aligned}
 \mathbf{F}_d &= \alpha \|\mathbf{A}_d - \mathbf{W}_d \mathbf{H}_d\|_F^2 + \|\mathbf{S}_d - \mathbf{W}_d \mathbf{W}_d^T\|_F^2, \\
 &\text{which is equivalent to, (recall (9))} \\
 &\alpha \|\mathbf{A}_d - \mathbf{W}_d \mathbf{H}_d\|_F^2 + \text{tr}(\mathbf{W}_d^T \mathbf{L}_d \mathbf{W}_d) \\
 &= \alpha \sum_{i=1}^d \sum_{j=1}^p ((\mathbf{A}_d)_{ij} - (\mathbf{W}_d \mathbf{H}_d)_{ij})^2 + \sum_{k=1}^K \sum_{i=1}^d \sum_{j=1}^d (\mathbf{W}_d^T)_{ki} (\mathbf{L}_d)_{ij} (\mathbf{W}_d)_{jk} \\
 &= \left[\alpha \sum_{i=1}^{d-1} \sum_{j=1}^p ((\mathbf{A}_{d-1})_{ij} - (\mathbf{W}_{d-1} \mathbf{H}_d)_{ij})^2 + \sum_{k=1}^K \sum_{i=1}^{d-1} \sum_{j=1}^{d-1} (\mathbf{W}_{d-1}^T)_{ki} (\mathbf{L}_d)_{ij} (\mathbf{W}_{d-1})_{jk} \right] \\
 &+ \left[\alpha \sum_{j=1}^p ((\mathbf{a}_d)_j - (\mathbf{w}_d \mathbf{H}_d)_j)^2 + \sum_{k=1}^K \sum_{i=1}^{d-1} (\mathbf{W}_d^T)_{ki} (\mathbf{L}_d)_{id} (\mathbf{w}_d)_k + \sum_{k=1}^K \sum_{j=1}^{d-1} (\mathbf{w}_d^T)_k (\mathbf{L}_d)_{dj} (\mathbf{W}_d)_{jk} \right. \\
 &\left. + \sum_{k=1}^K (\mathbf{w}_d^T)_k (\mathbf{L}_d)_{dd} (\mathbf{w}_d)_k \right] \\
 &= \mathbf{F}_{d-1} + \mathbf{f}_d.
 \end{aligned} \tag{12}$$

Appatently, the NS-NMF objective function in (12) is divided into two parts— \mathbf{F}_{d-1} denotes the cost up to the $(d-1)$ th sample and \mathbf{f}_d denotes the cost of the d th sample, whereas \mathbf{w}_d and \mathbf{a}_d denote, respectively, the last row of \mathbf{W}_d and \mathbf{A}_d . This strategy is known as the incremental NMF in the literature (Sun et al., 2018; Chen et al., 2018; Zhang et al., 2019). As the number of samples increases, new observations will have minor influence on the basis matrix, so that updating only the weight vector of the last sample will suffice.

In light of this thought, we can consider the first $d-1$ rows of \mathbf{W}_d equal to \mathbf{W}_{d-1} . To compute the cost of d th sample, i.e., \mathbf{f}_d , we need to establish an updating policy for the basis matrix component $(\mathbf{H}_d)_{kj}$ and weight matrix component $(\mathbf{w}_d)_k$. We can utilize the gradient descent approach to derive the update policy as following:

$$(\mathbf{w}_d)_k^{t+1} = (\mathbf{w}_d)_k^t - \delta_k \frac{\partial \mathbf{F}_d}{\partial (\mathbf{w}_d)_k^t}, \tag{13}$$

$$(\mathbf{H}_d)_{kj}^{t+1} = (\mathbf{H}_d)_{kj}^t - \theta_{kj} \frac{\partial \mathbf{F}_d}{\partial (\mathbf{H}_d)_{kj}^t}. \tag{14}$$

In (13) and (14), δ and θ denote the step sizes, t denotes the iteration number, $k = 1, 2, \dots, K$, and $j = 1, 2, \dots, p$. The step sizes are chosen as in (15) and (16), following the work in Cai et al. (2011) and Guan et al. (2012):

$$\delta_k = \frac{(\mathbf{w}_d)_k^t}{2(\alpha((\mathbf{w}_d)_k^t \mathbf{H}_d^t (\mathbf{H}_d^t)^T + \sum_{i=1}^d (\mathbf{D}_d)_{id} \mathbf{w}_i^t))_k}, \tag{15}$$

$$\theta_{kj} = \frac{(\mathbf{H}_d)_{kj}^t}{2\alpha(\mathbf{W}_{d-1}^T \mathbf{W}_{d-1} \mathbf{H}_d^t + (\mathbf{w}_d^{t+1})^T \mathbf{w}_d^{t+1} \mathbf{H}_d^t)_{kj}}. \tag{16}$$

Substituting (15) and (16) into (12) and (13), we obtain the updating policy as follows:

$$(\mathbf{w}_d)_k^{t+1} = (\mathbf{w}_d)_k^t \frac{(\alpha a_d (\mathbf{H}_d^t)^T + \sum_{i=1}^{d-1} (\mathbf{S}_d)_{id} \mathbf{w}_i^t)_k}{(\alpha (\mathbf{w}_d)^t \mathbf{H}_d^t (\mathbf{H}_d^t)^T + (\mathbf{D}_d)_{dd} \mathbf{w}_d^t)_k}, \quad (17)$$

$$(\mathbf{H}_d)_{kj}^{t+1} = (\mathbf{H}_d)_{kj}^t \frac{(\mathbf{W}_{d-1}^T \mathbf{A}_d + (\mathbf{w}_d^{t+1})^T \mathbf{a}_d)_{kj}}{(\mathbf{W}_{d-1}^T \mathbf{W}_{d-1} \mathbf{H}_d^t + (\mathbf{w}_d^{t+1})^T \mathbf{w}_d^{t+1} \mathbf{H}_d^t)_{kj}}, \quad (18)$$

where \mathbf{S}_d and \mathbf{D}_d represent, respectively, the MST based weight matrix and degree matrix.

If we look at (18), it requires all the data samples before the d th one to compute the update but doing so will significantly increase the memory requirements. To overcome the problem, we can use the strategy of cumulative summation. Let us first introduce two variables \mathbf{U}_d and \mathbf{V}_d with initial values $\mathbf{U}_0 = \mathbf{V}_0 = \mathbf{0}$. Then using (19) and (20), we can rewrite the update policy for \mathbf{H}_d as in (21) which now no longer needs to memorize all the samples.

$$\begin{aligned} \mathbf{U}_d &= \sum_{i=1}^d \mathbf{w}_i^T \mathbf{w}_i \\ &= \mathbf{U}_{d-1} + \mathbf{w}_d^T \mathbf{w}_d \end{aligned} \quad (19)$$

$$\begin{aligned} \mathbf{V}_d &= \sum_{i=1}^d \mathbf{w}_i^T \mathbf{a}_i \\ &= \mathbf{V}_{d-1} + \mathbf{w}_d^T \mathbf{a}_d \end{aligned} \quad (20)$$

$$(\mathbf{H}_d)_{kj}^{t+1} = (\mathbf{H}_d)_{kj}^t \frac{(\mathbf{V}_d)_{kj}}{\mathbf{U}_d (\mathbf{H}_d^t)_{kj}} \quad (21)$$

Another problem with (17) is that in order to update $(\mathbf{w}_d)_k$, we need to reconstruct the MST with all the data samples every time as a new sample comes in. Again, doing so slows down the online operation. To address this problem we adopt the combination of local MST (Ahmed et al., 2019a) and buffering strategy (Goldberg et al., 2008; Liu et al., 2016). In a local MST, for each observation we construct a MST with its neighbors only. These neighbors can be chosen in a temporal fashion. In other words, the neighbors of the d th sample (which just arrives) are the samples having arrived in a specified time window before it, say, in the window of dating back to time instance $d - z$, where z is the size of the time window. If $z = 50$, it means that the MST will be constructed based on the d th sample and the most recent 50 samples arrived before the d th sample. The buffering strategy states that instead of discarding all the old data samples, one maintains a buffer of specified size, Q . After the buffer is full for the first time, any new sample will be added to the buffer while the buffer drops the oldest one and thereby keeps its size the same. To connect the two approaches, we set the time window size the same as the buffer size, i.e., $Q = z$. Consequently, we can rewrite the updating policy for $(\mathbf{w}_d)_k$ as

$$(\mathbf{w}_d)_k^{t+1} = (\mathbf{w}_d)_k^t \frac{(\alpha \mathbf{a}_d (\mathbf{H}_d^t)^T + \sum_{i=d-z}^{d-1} (\mathbf{S}_d)_{id} \mathbf{w}_i^t)_k}{(\alpha (\mathbf{w}_d)^t \mathbf{H}_d^t (\mathbf{H}_d^t)^T + (\mathbf{D}_d)_{dd} \mathbf{w}_d^t)_k}. \quad (22)$$

Algorithm 2: Online implementation of NS-NMF algorithm for anomaly detection

Input : Current observation, \mathbf{a}_d , trade-off parameter, α , buffer size, z , and the number of clusters, K
Output: Current basis matrix, \mathbf{H}_d , and anomaly score, O_d

- 1 Initialize \mathbf{H}_0 with random values;
- 2 Initialize $\mathbf{U}_0 = \mathbf{V}_0 = \mathbf{0}$;
- 3 Initialize $\mathbf{A}_0 = \mathbf{W}_0 = \mathbf{S}_0 = \phi$;
- 4 **while** a new observation \mathbf{a}_d arrives **do**
- 5 Draw the current sample \mathbf{a}_d ;
- 6 Initialize weight coefficient \mathbf{w}_d with random values;
- 7 Append \mathbf{a}_d to \mathbf{A}_{d-1} and assign it to \mathbf{A}_d ;
- 8 Append \mathbf{w}_d to \mathbf{W}_{d-1} and assign it to \mathbf{W}_d ;
- 9 **if** $d = z$ **then**
- 10 Construct MST using the observations in \mathbf{A}_d and store the weights in \mathbf{S}_d ;
- 11 Apply offline NS-NMF to obtain \mathbf{W}_d and \mathbf{H}_d ;
- 12 Calculate \mathbf{U}_d and \mathbf{V}_d using (19) and (20);
- 13 **end**
- 14 **if** $d > z$ **then**
- 15 Construct MST using the observations in \mathbf{A}_d and obtain \mathbf{s}_d ;
- 16 **repeat**
- 17 Use (22) to update \mathbf{w}_d^{t+1} using \mathbf{s}_d and \mathbf{H}_d ;
- 18 Use (19) and (20) to update \mathbf{U}_d and \mathbf{V}_d with \mathbf{w}_d^{t+1} ;
- 19 Use (22) to update \mathbf{H}_d^{t+1} ;
- 20 **until** Convergence;
- 21 Delete the first row vector from both \mathbf{A}_d and \mathbf{W}_d ;
- 22 Calculate the anomaly score for the d th observation using (23) and store it in O_d
- 23 **end**
- 24 **end**

The algorithm steps are summarized in Algorithm 2. There are three phases of the algorithm, after the initialization, we proceed to these phases. Steps 5–8 summarizes the first phase, i.e., $d < z$, where the new samples are added along with initialization of the weight vectors. When the buffer is full for the first time, i.e., $d = z$, it starts the second phase, in which an MST is constructed and the offline NS-NMF algorithm helps obtain the weights and basis vectors. Step 9–13 summarizes this phase. After that, the algorithm enters the third and final phase, i.e., $d > z$, where the update of the weight and basis vectors and calculation of the anomaly scores are carried out from Steps 14–23. In this phase, a gradient descent approach is used to obtain the updated weight and basis values for each new sample. Steps 16–20 summarizes the iterations on t , which are required for the convergence of gradient descent approach.

Similar to the offline counterpart, the assignment of an observation to the k th cluster is made according to the largest entry in \mathbf{w}_d . After that, we can compute the anomaly score

of the d th observation as in (23). Now, we can either choose a threshold and mark the observation as anomaly on the fly if its anomaly score crosses the threshold or we can store the anomaly scores to do the evaluation later. In this work, we test both of the options. For the benchmark datasets, which do not have any timestamps marking, we decide to go for the second option. What this means is that while we run the online algorithm to get the anomaly scores on the fly from the streaming data, the declaration of anomaly is again based on selecting the top N scores as anomalies, same as we do in our offline scenario. On the other hand, for the hydropower dataset, we do have the associated timestamps and therefore we know the order of the observations. So, we decide to go with the first option and mark anomalies on the fly.

$$O_d = \|\mathbf{a}_d - (\mathbf{H}_d)_k\|_2 \quad \text{when observation } d \text{ belongs to local community } k. \quad (23)$$

5. Comparative Performance Analysis of NS-NMF

We want to evaluate the performance of the proposed NS-NMF method for anomaly detection compared to the original NMF as well as GNMF and SNMF. In Section 5.1, we use 20 benchmark anomaly detection datasets from the study of Campos et al. (2016) for our performance comparison study. In Table 1, we summarize the basic characteristics of these 20 datasets. For all the benchmark datasets, the label of the observations whether it is normal or anomalous is known beforehand. There are several versions of these datasets available depending on the data cleaning and preprocessing steps involved. For our analysis we choose to use the normalized version of the datasets with all missing values removed and categorical variables are converted into numerical format. In Section 5.2, we apply the competitive methods to a real-life dataset from a hydropower plant.

To evaluate the performance of the methods, the criterion we use is called *precision at N* (Campos et al., 2016, $P@N$), which is a rather common performance metric used in anomaly detection. As we mention earlier, in a practical setting for anomaly detection, researchers often set a cut-off threshold N and flag the observations with the top- N anomaly scores, however it is defined and computed in respective methods. Ideally, N is chosen to be the number of true anomalies. Practically, N is chosen to be larger than the perceived number of anomalies but small enough to make the subsequent identification operations feasible.

In the benchmark study, since we know the number of true anomalies, we therefore use that value as our choice of N and treat it as the same cut-off for all methods in comparison. Because N is the number of true anomalies, the number of false alarms is implied, which is $N - N \times P@N$. That is why in the benchmark study, we only present $P@N$. In reality, when the number of true anomalies is not known, the main objective in anomaly detection is still to increase $P@N$ for a fixed N , i.e., to have a higher detection rate within the cut-off threshold.

The $P@N$ is defined as the proportion of correct anomalies identified in the top N ranks. For a dataset DB of size n , consisting of anomaly set $O \subset DB$ and normal datasets $I \subseteq DB$, such that $DB = O \cup I$, $P@N$ can be formulated as

$$P@N = \frac{\#\{o \in O \mid \text{rank}(o) \leq N\}}{N}, \quad \text{where } N = |O|. \quad (24)$$

Table 1: Public benchmark datasets used in the performance evaluation study.

Dataset	Number of observations (n)	Number of anomalies ($ O $)	Number of attributes (p)
Anthyroid	7,200	347	21
Arrhythmia	450	12	259
Cardiotocography	2,126	86	21
HeartDisease	270	7	13
Page Blocks	5,473	99	10
Parkinson	195	5	22
Pima	768	26	8
SpamBase	4,601	280	57
Stamps	340	16	9
WBC	454	10	9
Waveform	3,443	100	21
WPBC	198	47	33
WDBC	367	10	30
ALOI	50,000	1,508	27
KDDcup99	60,632	200	41
Shuttle	1,013	13	9
Ionosphere	351	126	32
Glass	214	9	7
Pen digits	9,868	20	16
Lymphography	148	6	19

Next, let us take a look at the parameter selection policies for the competing methods. The number of latent features or clusters, K is needed for all of the NMF-based methods. In this study we use $K = 5$. We have also explored the possibility of using $K = 2, 10, 15, 20$ and 25 and found that the relative performance of the competing methods remain the same in all cases. Based on our experiments with different K 's, we observe that the NMF-based anomaly detection methods perform better when K is in the range of $5 - 15$. We settle for $K = 5$ because it results in overall good detection performances for all competing methods. The cut-off value, N , required to generate the final anomaly list for both offline and online version, is taken as the number of true anomalies in the benchmark dataset studies, as discussed above. Other than these two parameters that are common to all methods, the rest of the parameters are algorithm-specific. We summarize the parameter choices in Table 2. For SNMF and GNMF, we adopt the best settings described in their original papers. For NS-NMF, as mentioned earlier, its performance is not sensitive to the choice of α . We settle at $\alpha = 0.8$ by conducting a few simple trials.

5.1 Performance Comparison using Public Available Datasets

We present the comparison of detection performance of the four offline methods on the 20 benchmark datasets in Table 3. For this comparison, we only consider the offline version of NS-NMF because the competitors are offline, so it is a bit unfair if we compare the online

Table 2: Parameter values and settings used for NS-NMF, GNMF and SNMF.

Competing methods	Number of latent factors, K	Other settings
Offline NS-NMF	5	Parameter controlling the influence of NMF, $\alpha = 0.8$ Regularizer for controlling overfitting, $\gamma = 0.2$
Online NS-NMF	5	Parameter controlling the influence of NMF, $\alpha = 0.8$ Buffer size, $z = B = 20$
GNMF	5	Manifold regularizer, $\lambda = 100$ Neighborhood graph construction parameter, $q = 5$ Weighting scheme for adjacency matrix: 0 – 1
SNMF	5	Gaussian similarity measure for constructing \mathbf{S}

Table 3: Performance comparison.

Anomaly detection methods	NS-NMF	NMF	GNMF	SNMF
	Performance (number of datasets)			
Better (uniquely best result)	12	0	0	2
Equal (equal to the existing best result)	6	3	4	4
Close (within 20% of the best result)	0	4	2	4
Worse (not within 20% of the best result)	2	13	14	10
Mean relative rank	1.1	3.0	2.6	2.2

version of NS-NMF. For this reason, NS-NMF means the offline NS-NMF in the comparison shown in Table 3, Table 4, and Figure 2.

To better reflect the methods’ comparative edge, we break down the comparison into four major categories in Table 3, namely *Better*, *Equal*, *Close* and *Worse*, as explained in the table. NS-NMF outperforms other methods by showing uniquely best detection performance on 12 out of 20 datasets and tying for the best in another six cases. Only in two cases NS-NMF is obviously worse than the best performer. SNMF achieves the uniquely best performance in those two cases, while NMF and GNMF tie for some best performance but never beat others outright. If we rank each of these four methods in a scale of 1 (best) to 4 (worst), then the mean rank for NS-NMF is 1.1, which is far ahead of other methods, with SNMF at 2.2 mean rank, GNMF 2.6 mean rank, and NMF 3.0 mean rank.

We apply the Friedman test, a non-parametric method (Demšar, 2006), to determine whether NS-NMF achieve significant improvement over other competitors. Let n_a be the number of anomaly detection methods and n_d be the number of datasets. We define a matrix Ra whose entries in each row represent the detection method’s rank for that specific dataset. If there are tied values, we assign to each tied value the average of the ranks that would have been assigned without ties. For example, suppose we have two tied methods both with rank 1. Had there been no tie, one should have been assigned rank 1 and the other rank 2. An Friedman test then uses the average of the two ranks, which is 1.5, as the rank value for both of these methods. Under the null hypothesis that all methods perform

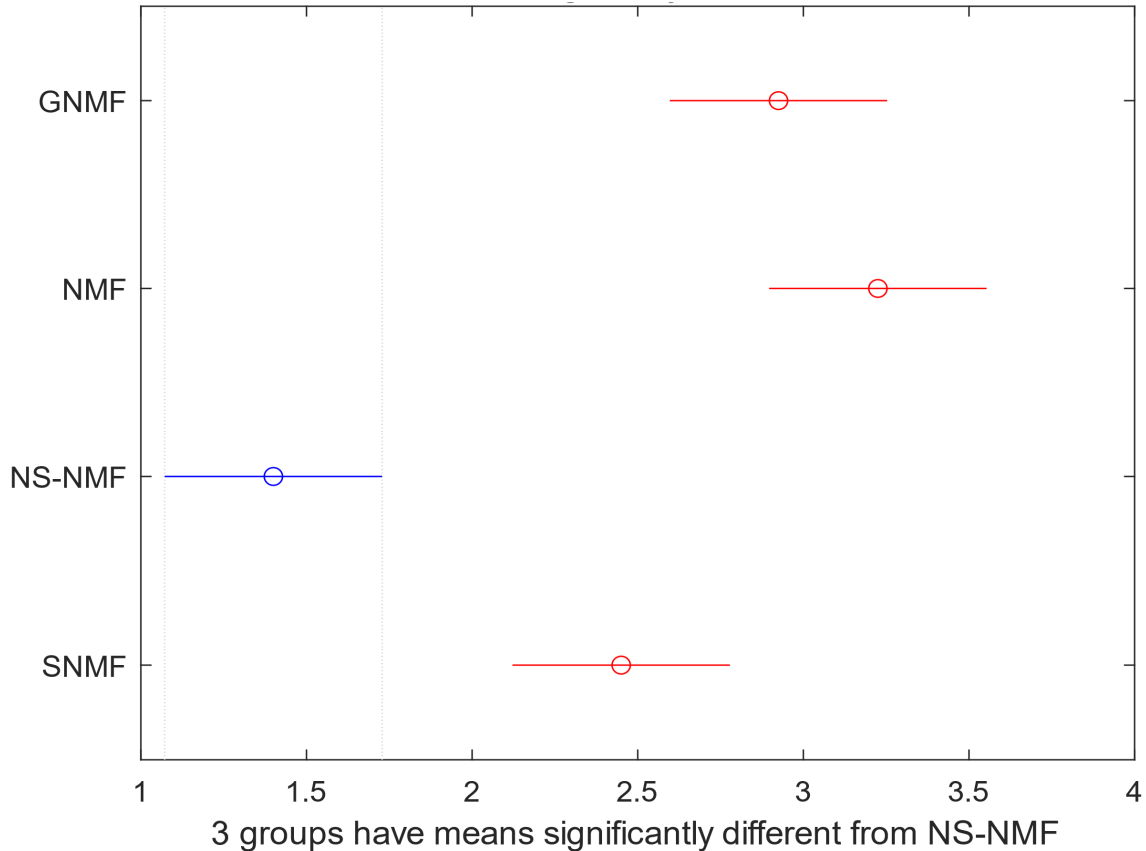


Figure 2: Post hoc analysis on the ranking data obtained by the Friedman test.

the same, the Friedman statistic,

$$\chi_F^2 = \frac{12n_d}{n_a(n_a + 1)} \left(\sum_{l=1}^{n_a} \overline{Ra}_l^2 - \frac{n_a(n_a + 1)^2}{4} \right), \quad (25)$$

follows a Chi-squared distribution with $n_a - 1$ degrees of freedom, where \overline{Ra}_l is the average value of column $l = 1, 2, \dots, n_a$. We found the p-value (4.11×10^{-6}) significant enough to reject the null hypothesis.

We also perform a post hoc analysis of the four methods in terms of their ranking performance. Fig. 2 presents the post hoc analysis on the ranking data and it indicates that ranking of NS-NMF is significantly better than the other three approaches at the 0.05 level of significance. The detailed pairwise comparisons between NS-NMF and each of the three methods are presented in Table 4. The p-values are calculated using the Conover post-hoc test (Conover, 1999). We employ the Bonferroni correction (Bland and Altman, 1995) to adjust the p-values for multiple comparisons. All the pairwise comparisons show a sufficiently significant difference.

Table 4: The p-values of pairwise comparisons between the NS-NMF method with each of the three competing methods.

Competing methods	p-value
NS-NMF vs NMF	1.64×10^{-18}
NS-NMF vs GNMF	2.86×10^{-15}
NS-NMF vs SNMF	1.20×10^{-9}

In Table 5, we summarize the number of true detections by the competing methods. We notice that the offline NS-NMF either outperforms or is no worse than NMF and GNMF in every single case. GNMF performs worse than the regular NMF in four cases. We use the best parameter setting for GNMF as recommended by its authors. We do observe the sensitive nature of GNMF to its parameters and acknowledge the possibility that some other parameter combinations might produce a better outcome. However, parameter selection in unsupervised learning settings is a difficult task, as the common approaches working well for supervised learning like cross validation does not work in the unsupervised circumstances. Therefore, the sensitivity of GNMF is certainly a shortcoming. SNMF’s performance is better than that of NMF and GNMF, although still overall worse than the offline NS-NMF. SNMF is the slowest in terms of computational time and it does not appear scalable on big datasets. For example, in the case of the ALOI dataset that has 50,000 observations, SNMF takes almost eight hours to generate the index of the anomalous observations, whereas offline NS-NMF takes one quarter of that time to complete the task, with the majority of its time spent on MST construction. NMF and GNMF are much faster and take around 12 mins and 35 mins, respectively, in processing the same dataset.

Here we also include the results from the online version of NS-NMF because we would like to draw a comparison between the offline and online NS-NMF and see how much efficiency the online NMF maintains while using a small subset of data to compute the anomaly scores. Unsurprisingly, the offline version comes out superior in 14 out of the 20 cases. On the other hand, for most of the cases with the exception of the case of **Annthyroid**, the online version does not perform that much worse than the offline version and never comes out as the uniquely worst performer among the methods. A bit surprisingly, the online version even beats its offline counterpart in three cases. It seems to suggest that in some cases, having a longer memory and global data connection may hurt the detection. Overall we deem the online NS-NMF a competent and promising online anomaly detection algorithm.

5.2 Application to a Power Plant Example

The industry dataset used in this study comes from a hydropower plant. The same dataset has been analyzed in our previous work (Ahmed et al., 2019a, 2018). To quickly recap the basic information of the dataset, we have a total of seven months worth of data, coming from different functional areas of the plant (turbines, generators, bearings etc.). We combine all the data from different functional areas according to their time stamps and perform some simple cleaning, statistical analysis and pre-processing; additional details about the data pre-processing can be found in Ahmed et al. (2018). In the end, we have $n = 9,219$ obser-

Table 5: Number of true positive detections of the competing methods. Bold entries represent the best detection performance in a respective dataset.

Dataset	Offline NS-NMF	Online NS-NMF	NMF	GNMF	SNMF
WBC	9	7	8	8	7
Waveform	6	31	0	1	26
Heart	4	4	3	4	4
WDBC	8	6	8	6	7
Glass	4	1	0	0	1
Spambase	36	38	21	23	28
WPBC	16	11	11	11	13
Stamps	5	2	1	2	4
Parkinson	3	3	2	3	2
Lymphography	5	3	5	3	5
Ionosphere	82	68	51	38	65
PIMA	9	4	8	3	2
Shuttle	4	1	1	1	3
Cardiotocography	19	11	13	19	33
Arrhythmia	5	3	3	3	3
Page blocks	38	38	24	38	38
Pendigits	0	1	0	0	0
KDD	87	81	56	82	78
ALOI	151	121	91	97	84
Anthyroid	40	18	13	12	24

vations and $p = 222$ attributes. Then we apply NS-NMF, GNMF and SNMF algorithms to find out the anomalies in this dataset. We use the same parameter settings as we do in the benchmark dataset study. The only difference is that we no longer have the information of the number of true anomalies. After consulting the operating manager who provided this dataset, we are advised to report top 100 anomalous time stamps to the manager. The manager would follow up and check the status of operation in detail, for instance, by manually examining operational logs and physical conditions of components, and then confirm us about the validity of the findings.

The top 100 anomalies identified by the three methods are shown in Table 6. We use both online and offline version of NS-NMF. To detect anomalies on the fly, we use the threshold update policy similar to (Ahmed et al., 2019b) for the online algorithm. To save space we skip some rows in the table. We observe that altogether these three methods have 33 common anomalous time stamps among the top 100 anomalies, whereas offline NS-NMF, online NS-NMF and GNMF produce similar outcomes and share 49 common time stamps. These common findings serve as an indirect way of cross validating the sanity of the detection outcomes.

Apart from the common detection outcomes, we find that the anomalous time stamps belong to a few anomaly-prone days, which are listed in Table 7. It is also noticeable that

Table 6: Summary of the top 100 anomalies.

Offline NS-NMF	Online NS-NMF	GNMF	SNMF
7/4/2015 11:30	7/4/2015 11:50	7/4/2015 11:30	4/15/2015 16:50
7/4/2015 11:40	7/4/2015 12:00	7/4/2015 11:40	4/15/2015 18:30
7/4/2015 11:50	7/4/2015 12:20	7/4/2015 11:50	4/15/2015 20:10
7/4/2015 12:00	7/4/2015 12:30	7/4/2015 12:00	4/15/2015 22:30
7/4/2015 12:10	7/4/2015 12:50	7/4/2015 12:10	4/15/2015 22:50
7/4/2015 12:20	7/4/2015 1:00	7/4/2015 12:20	4/16/2015 2:50
7/4/2015 12:30	7/4/2015 1:30	7/4/2015 12:30	4/16/2015 4:30
.....
9/13/2015 19:00	9/14/2015 7:40	7/4/2015 14:40	4/18/2015 23:10
9/14/2015 2:40	9/14/2015 7:50	7/8/2015 12:20	4/19/2015 4:00
9/14/2015 8:00	9/14/2015 8:00	7/8/2015 18:00	4/19/2015 21:40
9/14/2015 8:10	9/14/2015 8:10	9/15/2015 21:20	4/19/2015 23:40
9/14/2015 8:20	9/14/2015 8:20	9/15/2015 21:40	4/20/2015 8:20
9/14/2015 8:30	9/14/2015 8:30	10/3/2015 18:50	7/4/2015 11:30
9/14/2015 13:00	9/14/2015 8:50	10/3/2015 19:10	7/4/2015 11:50
9/14/2015 13:10	9/14/2015 13:00	10/3/2015 19:20	7/4/2015 12:00
.....
10/3/2015 20:50	10/3/2015 20:20	10/3/2015 22:20	7/4/2015 15:00
10/3/2015 21:00	10/3/2015 20:30	10/3/2015 22:30	7/4/2015 15:10
10/3/2015 21:10	10/3/2015 20:40	10/3/2015 22:40	7/4/2015 15:20
10/3/2015 21:20	10/3/2015 20:50	10/3/2015 22:50	7/4/2015 15:30
10/3/2015 21:30	10/3/2015 21:30	10/3/2015 23:00	7/4/2015 15:40
10/3/2015 21:40	10/3/2015 21:50	10/3/2015 23:10	7/4/2015 15:50
10/3/2015 21:50	10/3/2015 21:20	10/3/2015 23:20	7/4/2015 16:00
.....
10/4/2015 0:00	10/3/2015 23:40	10/4/2015 17:20	7/4/2015 18:10
10/4/2015 0:10	10/3/2015 23:50	10/4/2015 17:30	7/8/2015 12:20
10/4/2015 0:20	10/4/2015 0:00	10/4/2015 17:40	7/8/2015 15:50
10/4/2015 23:40	10/4/2015 0:10	10/4/2015 17:50	7/8/2015 18:00
10/4/2015 23:50	10/4/2015 0:20	10/4/2015 18:00	9/17/2015 4:40
10/5/2015 1:00	10/4/2015 0:30	10/4/2015 18:10	9/17/2015 4:50
10/5/2015 1:30	10/4/2015 22:50	10/4/2015 18:20	9/17/2015 5:00
.....
10/5/2015 4:30	10/13/2015 17:25	10/5/2015 3:30	10/3/2015 20:40
10/5/2015 4:40	10/13/2015 17:30	10/5/2015 3:40	10/3/2015 21:50
10/5/2015 4:50	10/13/2015 17:35	10/5/2015 3:50	10/3/2015 22:00
10/13/2015 16:35	10/13/2015 17:45	10/5/2015 4:00	10/3/2015 22:10
10/13/2015 16:45	10/13/2015 18:20	10/5/2015 4:10	10/3/2015 22:20
10/13/2015 16:55	10/13/2015 18:30	10/5/2015 4:20	10/3/2015 22:30
.....
1/2/2016 21:20	1/11/2016 18:10	10/13/2015 17:05	10/13/2015 17:25
1/2/2016 21:30	1/12/2016 11:20	10/13/2015 17:15	10/13/2015 17:35
1/2/2016 21:40	1/12/2016 11:30	10/13/2015 17:25	10/13/2015 17:45
1/12/2016 11:20	1/12/2016 11:40	10/13/2015 17:35	10/14/2015 18:35
1/12/2016 11:30	1/12/2016 12:10	10/13/2015 17:45	1/3/2016 7:00

Table 7: Most anomaly prone days identified by the three methods.

July 4 th , 2015
September 13 th , 2015
September 14 th , 2015
October 3 rd , 2015
October 5 th , 2015
October 13 th , 2015
October 14 th , 2015
January 2 nd , 2016
January 12 th , 2016

anomalies occur in chunks, and in most cases, the observations in the close time vicinity of an anomalous time stamp are also returned as anomalies. When we report these time stamps to the operating manager, he agrees, after his own verification, that most of these findings present valid concerns and indeed require trouble shooting.

While there is a good common ground shared by these methods, the competing methods do perform differently at certain aspect. Despite the close performance between GNMF and NS-NMF, GNMF entirely misses the anomalous stamps on September 13th, September 14th, January 2nd, and January 12th. SNMF likewise misses those dates but does detect one time stamp on January 12th. The offline NS-NMF successfully identified all of those time stamps, but misses some potential anomalous time stamps in the month of April, and so does the online NS-NMF. The online NS-NMF also misses the anomalies on September 13th and January 2nd. SNMF successfully detects the April dates. All of them misses the January 9th anomalies which are deemed as abnormal by the operating manager and his team. The operating manager also indicate that July 8th, September 17th, January 3rd time stamps do not appear to be anomalies, after their extensive closer-look that yields no intelligible outcomes. These dates are identified as anomalous by SNMF but not by NS-NMF or GNMF. The operating manager registers the offline version of NS-NMF as the most competitive method followed by the online counter part among the competitors.

Detecting the anomalies does not tell us directly the root cause behind the abnormal behaviors. But anomaly detection outcomes can be used to assign class labels to the respective data records. A simple follow-up is to build a classification and regression tree on the labeled datasets, which can reveal which variable, or variable combination, is actually leading to these anomalous conditions. Doing so injects the interpretability to an unsupervised learning problem and can advise proper actions to address the anomalous condition and prevent future damage, disruption, or even catastrophe. An example of such exercise can be found in Ahmed et al. (2019a, 2018) and we will not repeat it here.

6. Summary

In this paper, we propose a neighborhood structure-assisted non-negative matrix factorization method and demonstrate its application in anomaly detection. We argue that in the absence of the similarity information, the original NMF basis vectors are not enough to represent and separate complicated clusters in the reduced feature space. To represent

and summarize the complex data structure information in a similarity matrix, we use a minimum spanning tree to capture the neighborhood connectivity information and to approximate the geodesic distance between data instances. The current approaches that use Euclidean distance based similarity metric is not capable of approximating the true data space structure and those approaches using the complete graphs become computationally expensive. We develop a joint optimization framework to obtain the clustering indicator and the attribute distribution matrix, and then, we devise an anomaly score to flag potential point-wise anomalies. We use a parallel block stochastic gradient descent method to compute these factored matrices for fast implementation. We also design an online algorithm to render the proposed method applicable in analyzing streaming data. The specific action of modeling the neighborhood structure appears to make an appreciable impact, as NS-NMF demonstrates clear advantage in the task of anomaly detection in an extensive empirical study using 20 benchmark datasets and one hydropower dataset.

Acknowledgments

Imtiaz Ahmed and Yu Ding were partially supported by grants from NSF under grant no. CMMI-1545038 and ABB project contract no. M1801386. Xia Ben Hu was partially supported by NSF grants (IIS-1750074 and IIS-1718840).

References

- Imtiaz Ahmed, Aldo Dagnino, Alessandro Bongiovi, and Yu Ding. Outlier detection for hydropower generation plant. In *Proceedings of the 14th IEEE International Conference on Automation Science and Engineering*. IEEE, 2018.
- Imtiaz Ahmed, Aldo Dagnino, and Yu Ding. Unsupervised anomaly detection based on minimum spanning tree approximated distance measures and its application to hydropower turbines. *IEEE Transactions on Automation Science and Engineering*, 16(2):654–667, 2019a. doi: 10.1109/TASE.2018.2848198.
- Imtiaz Ahmed, Travis Galoppo, and Yu Ding. O-LoMST: An online anomaly detection approach and its application in a hydropower generation plant. In *Proceedings of the 15th IEEE International Conference on Automation Science and Engineering*. IEEE, 2019b.
- Edward G. Allan, Michael R. Horvath, Christopher V. Kopek, Brian T. Lamb, Thomas S. Whaples, and Michael W. Berry. Anomaly detection using nonnegative matrix factorization. In *Survey of Text Mining II*, pages 203–217. Springer, 2008.
- Mennatallah Amer and Markus Goldstein. Nearest-neighbor and clustering based anomaly detection algorithms for rapidminer. In *Proceedings of the 3rd RapidMiner Community Meeting and Conference*, pages 1–12. RCOMM, 2012.
- John M. Bland and Douglas G. Altman. Multiple significance tests: the Bonferroni method. *BMJ*, 310:170, 1995.

- Deng Cai, Xiaofei He, Jiawei Han, and Thomas S. Huang. Graph regularized nonnegative matrix factorization for data representation. *IEEE Transactions on Pattern Analysis and Machine Intelligence*, 33(8):1548–1560, 2011.
- Guilherme O. Campos, Arthur Zimek, Jörg Sander, Ricardo JGB Campello, Barbora Mícenková, Erich Schubert, Ira Assent, and Michael E. Houle. On the evaluation of unsupervised outlier detection: measures, datasets, and an empirical study. *Data Mining and Knowledge Discovery*, 30(4):891–927, 2016.
- Zigang Chen, Lixiang Li, Haipeng Peng, Yuhong Liu, and Yixian Yang. Incremental general non-negative matrix factorization without dimension matching constraints. *Neurocomputing*, 311:344–352, 2018.
- William J. Conover. *Practical Nonparametric Statistics*. Wiley, 1999.
- Jose Costa and Alfred O. Hero. Manifold learning with geodesic minimal spanning trees. *arXiv:cs/0307038 [cs.CV]*, 2003.
- Janez Demšar. Statistical comparisons of classifiers over multiple data sets. *The Journal of Machine Learning Research*, 7:1–30, 2006.
- Chris Ding, Xiaofeng He, and Horst D. Simon. On the equivalence of nonnegative matrix factorization and spectral clustering. In *Proceedings of the 2005 SIAM International Conference on Data Mining*, pages 606–610. SIAM, 2005.
- Levent Ertöz, Eric Eilertson, Aleksandar Lazarevic, Pang-Ning Tan, Vipin Kumar, Jaideep Srivastava, and Paul Dokas. Minds – Minnesota intrusion detection system. In Hillol Kargupta, Jiawei Han, Philip S. Yu, Rajeev Motwani, and Vipin Kumar, editors, *Next Generation Data Mining*, chapter 3, pages 199–218. MIT Press Cambridge, MA, 2004.
- Martin Ester, Hans-Peter Kriegel, Jörg Sander, and Xiaowei Xu. A density-based algorithm for discovering clusters in large spatial databases with noise. In *Proceedings of the Second International Conference on Knowledge Discovery and Data Mining*, pages 226–231. ACM, 1996.
- Rainer Gemulla, Erik Nijkamp, Peter J. Haas, and Yannis Sismanis. Large-scale matrix factorization with distributed stochastic gradient descent. In *Proceedings of the 17th ACM SIGKDD International Conference on Knowledge Discovery and Data mining*, pages 69–77. ACM, 2011.
- Andrew B Goldberg, Ming Li, and Xiaojin Zhu. Online manifold regularization: A new learning setting and empirical study. In *Joint European Conference on Machine Learning and Knowledge Discovery in Databases*, pages 393–407. Springer, 2008.
- Naiyang Guan, Dacheng Tao, Zhigang Luo, and Bo Yuan. Online nonnegative matrix factorization with robust stochastic approximation. *IEEE Transactions on Neural Networks and Learning Systems*, 23(7):1087–1099, 2012.
- Zhibo Guo and Ying Zhang. A label-embedding online nonnegative matrix factorization algorithm. *IEEE Access*, 7:105882–105891, 2019.

- Zengyou He, Xiaofei Xu, and Shengchun Deng. Discovering cluster-based local outliers. *Pattern Recognition Letters*, 24(9):1641–1650, 2003.
- Fabian Keller, Emmanuel Muller, and Klemens Bohm. HiCS: High contrast subspaces for density-based outlier ranking. In *IEEE 28th International Conference on Data Engineering*, pages 1037–1048. IEEE, 2012.
- Hans-Peter Kriegel, Peer Kröger, Erich Schubert, and Arthur Zimek. Outlier detection in axis-parallel subspaces of high dimensional data. In *Advances in Knowledge Discovery and Data Mining: Proceedings of the 13th Pacific-Asia Conference on Knowledge Discovery and Data Mining*, pages 831–838. Springer, 2009.
- Da Kuang, Chris Ding, and Haesun Park. Symmetric nonnegative matrix factorization for graph clustering. In *Proceedings of the 2012 SIAM International Conference on Data Mining*, pages 106–117. SIAM, 2012.
- Daniel D. Lee and Hyunjune Sebastian Seung. Learning the parts of objects by non-negative matrix factorization. *Nature*, 401(6755):788–791, 1999.
- Fudong Liu, Xuejun Yang, Naiyang Guan, and Xiaodong Yi. Online graph regularized non-negative matrix factorization for large-scale datasets. *Neurocomputing*, 204:162–171, 2016.
- Ninghao Liu, Xiao Huang, and Xia Hu. Accelerated local anomaly detection via resolving attributed networks. In *Proceedings of the 26th International Joint Conference on Artificial Intelligence*, pages 2337–2343. AAAI Press, 2017.
- Emmanuel Müller, Ira Assent, Uwe Steinhausen, and Thomas Seidl. Outrank: ranking outliers in high dimensional data. In *IEEE 24th International Conference on Data Engineering Workshop*, pages 600–603. IEEE, 2008.
- Matthew E. Otey, Srinivasan Parthasarathy, Amol Ghoting, Guoqiang Li, Sundeep Naravula, and Dhableswar K. Panda. Towards NIC-based intrusion detection. In *Proceedings of the Ninth ACM SIGKDD International Conference on Knowledge Discovery and Data Mining*, pages 723–728. ACM, 2003.
- Robert C. Prim. Shortest connection networks and some generalizations. *Bell Labs Technical Journal*, 36(6):1389–1401, 1957.
- Jing Sun, Zhihui Wang, Haojie Li, and Fuming Sun. Incremental nonnegative matrix factorization with sparseness constraint for image representation. In *Pacific Rim Conference on Multimedia*, pages 351–360. Springer, 2018.
- Hanghang Tong and Ching-Yung Lin. Non-negative residual matrix factorization with application to graph anomaly detection. In *Proceedings of the 2011 SIAM International Conference on Data Mining*, pages 143–153. SIAM, 2011.
- Ding Tu, Ling Chen, Mingqi Lv, Hongyu Shi, and Gencai Chen. Hierarchical online nmf for detecting and tracking topic hierarchies in a text stream. *Pattern Recognition*, 76: 203–214, 2018.

- Wei-Chih Tu, Shengfeng He, Qingxiong Yang, and Shao-Yi Chien. Real-time salient object detection with a minimum spanning tree. In *The IEEE Conference on Computer Vision and Pattern Recognition*, pages 2334–2342. IEEE, 2016.
- Bas Van Stein, Matthijs Van Leeuwen, and Thomas Bäck. Local subspace-based outlier detection using global neighbourhoods. In *IEEE International Conference on Big Data*, pages 1136–1142. IEEE, 2016.
- Wei Xu, Xin Liu, and Yihong Gong. Document clustering based on non-negative matrix factorization. In *Proceedings of the 26th Annual International ACM SIGIR Conference on Research and Development in Informaion Retrieval*, pages 267–273. ACM, 2003.
- Dantong Yu, Gholamhosein Sheikholeslami, and Aidong Zhang. Findout: Finding outliers in very large datasets. *Knowledge and Information Systems*, 4(4):387–412, 2002.
- Meichen Yu, Arjan Hillebrand, Prejaas Tewarie, Jil Meier, Bob V. Dijk, Piet Van Mieghem, and Cornelis Jan Stam. Hierarchical clustering in minimum spanning trees. *Chaos: An Interdisciplinary Journal of Nonlinear Science*, 25(2):1–10, 2015.
- Ji Zhang, Meng Lou, Tok Wang Ling, and Hai Wang. HOS (high dimensional outlying subspace)-miner: a system for detecting outlying subspaces of high-dimensional data. In *Proceedings of the 30th International Conference on Very Large Data Bases*, pages 1265–1268. VLDB, 2004.
- Xiaoxia Zhang, Degang Chen, and Kesheng Wu. Incremental nonnegative matrix factorization based on correlation and graph regularization for matrix completion. *International Journal of Machine Learning and Cybernetics*, 10(6):1259–1268, 2019.
- Renbo Zhao and Vincent YF Tan. Online nonnegative matrix factorization with outliers. *IEEE Transactions on Signal Processing*, 65(3):555–570, 2016.
- Fei Zhu and Paul Honeine. Online kernel nonnegative matrix factorization. *Signal Processing*, 131:143–153, 2017.
- Arthur Zimek, Erich Schubert, and Hans-Peter Kriegel. A survey on unsupervised outlier detection in high-dimensional numerical data. *Statistical Analysis and Data Mining*, 5(5):363–387, 2012.